

RSC Advances



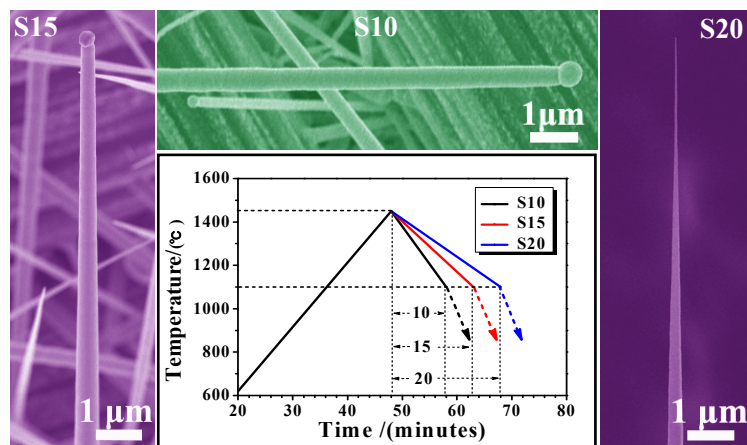
This is an *Accepted Manuscript*, which has been through the Royal Society of Chemistry peer review process and has been accepted for publication.

Accepted Manuscripts are published online shortly after acceptance, before technical editing, formatting and proof reading. Using this free service, authors can make their results available to the community, in citable form, before we publish the edited article. This *Accepted Manuscript* will be replaced by the edited, formatted and paginated article as soon as this is available.

You can find more information about *Accepted Manuscripts* in the [Information for Authors](#).

Please note that technical editing may introduce minor changes to the text and/or graphics, which may alter content. The journal's standard [Terms & Conditions](#) and the [Ethical guidelines](#) still apply. In no event shall the Royal Society of Chemistry be held responsible for any errors or omissions in this *Accepted Manuscript* or any consequences arising from the use of any information it contains.

Table of Contents Entry



We report the controlled growth of 3C-SiC flexible field emitters with clear and sharp tips based on the VLS mechanism.

Controlled Growth of SiC Flexible Field Emitters with Clear and Sharp Tips

Shanliang Chen^{1,2,3}, Pengzhan Ying², Lin Wang³, Fengmei Gao³, Guodong Wei³, Jinju Zheng³, Zhipeng Xie⁴, and Weiyu Yang^{3,}*

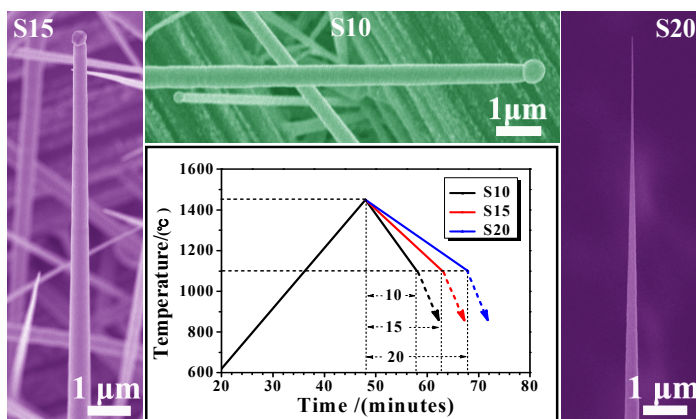
¹ School of Chemical Engineering and Technology, China University of Mining and Technology, Xuzhou City, 221116, P.R. China.

² School of Material Science and Engineering, China University of Mining and Technology, Xuzhou City, 221116, P.R. China.

³ Institute of Materials, Ningbo University of Technology, Ningbo City, 315016, P.R. China.

⁴ State Key Laboratory of New Ceramics and Fine Processing, Department of Materials Science and Engineering, Tsinghua University, Beijing, 100084, China

Graphical Table of Contents



We report the controlled growth of 3C-SiC flexible field emitters with clear and sharp tips based on the VLS mechanism.

* Corresponding author. E-mail: weiyuyang@tsinghua.org.cn (W. Yang)

Tel: +86-574-87080966, Fax: +86-574-87081221.

ABSTRACT

With respect to the effect of local field enhancement, fabrication of nanostructures with clear and sharp tips is critically important for the exploration of field emitters with high performances. In present work, aimed to the exploration of the flexible SiC field emitters with excellent properties, we report the controlled growth of quasialigned SiC nanoarrays with sharp tips via catalyst assisted pyrolysis of polymeric precursors on the carbon fabric substrates by tailoring the cooling rates. The resultant products are characterized by X-ray diffraction (XRD), scanning electron microscopy (SEM) and high-resolution transmission electron microscopy (HRTEM). It is found that the growth of SiC quasialigned nanoneedle arrays with unique sharp tips could be achieved by reducing the cooling rates over the high-temperature pyrolysis process, enabling the capability for the controlled growth of SiC flexible field emitters on carbon fabric. The cooling rates are optimized, which suggests that 17.5 °C/min is low enough to favor the growth of SiC nanowires with clear and sharp tips. The growth of the quasialigned SiC nanoarrays with sharp tips based on the typical VLS mechanism has been proposed. The FE property measurements suggest that the electron emission could be remarkably enhanced by tailoring the growth of SiC nanowires with clear and sharp tips.

1. Introduction

One-dimensional (1D) semiconductor nanostructures, owing to their unique geometries and excellent properties, have attracted extensive interest in the exciting and promising applications to be used as both interconnects and functional units for building opto/electrical nanodevices.¹⁻⁴ Among these 1D nano-sized semiconductor families, SiC 1D nanostructures are one of the most promising nanoscale building blocks and have been extensively studied in recent years,⁵⁻⁷ due to their excellent properties such as superior mechanical properties, high thermal conductivity, low thermal-expansion coefficient, good thermal-shock resistance, as well as its chemical stability and electron affinity, which allow them to be an excellent candidate to work in harsh environments.^{8,9} Thus, many efforts have been devoted to the growth and applications of SiC 1D nanostructures.¹⁰⁻¹²

One of the important applications of the SiC 1D nanostructures is to be utilized as the field emitter cathodes. Many previous works reported that SiC 1D nanostructures possess excellent electron emission properties with turn-on fields lower than $1 \text{ V}/\mu\text{m}$.¹³⁻¹⁹ There are three strategies for enhancing their field emission (FE) properties, *i.e.*, making the nanostructures with sharp tips,^{13,20} increasing the density of the emitting sites,²¹⁻²³ and tailoring the band gap of established nanomaterials via doping strategy.^{24,25} Due to the effect of local field enhancement, growth of the nanostructures with clear (without the attached catalytic droplets) and sharp tips (needle shaped) has been considered as one of the most efficient way for improving the FE properties.^{13,20,26,27} However, this is still a challenge for the fabrication of 1D nanostructures via the bottom-up route currently. Wang *et al.*²⁸ reported the tailored growth of the SiC nanowires with sharp tips base on vapor-liquid-solid (VLS) process by varying the pressure of the source species. They pointed out that the real-time controlled growth of the SiC

nanowires in the diameters could be achieved by tailoring the sizes of the catalytic droplets. Feng *et al.*²⁹ reported the precisely controlled growth of SiC nanowires based upon the VLS process by tailoring the cooling rates, which provided a novel strategy for well-controlled growth 1D semiconductor nanostructures.

In our previous work,²⁵ we report the growth of flexible N-doped SiC quasialigned nanoarrays on carbon fabric substrate with turn-on fields of 1.90~2.65 V/ μm and threshold field of 2.53~3.51 V/ μm , respectively. In current work, to further enhance the field emission properties of these flexible SiC field emitters, we report the growth of flexible SiC quasialigned nanoarrays with clear and sharp tips via catalyst assisted pyrolysis of polymeric precursors by tailoring the cooling rates during the high-temperature pyrolysis procedure. Meanwhile, the cooling rates are optimized, which favors the controlled growth of SiC flexible nanoneedle arrays with clear and sharp tips. The resultant SiC nanostructures, especially the SiC nanoneedles with clear and sharp tips, exhibit a very excellent FE performance. Present work could push forward the practical applications of SiC 1D nanostructures towards the field emitters with enhanced FE properties.

2. Experimental Procedure

The field emitters of quasialigned SiC nanoneedle arrays were synthesized by catalyst-assisted pyrolysis of polyureasilazane (Ceraset, Kion Corporation, USA) precursor in a graphite-heater furnace on the carbon fabric substrates. The polyureasilazane (PSN) was first solidified by heat-treatment at 260°C for 30 min under Ar atmosphere, and then subjected to be ball-milled into powders. Carbon fabric substrates were immersed into the ethanol solution of $\text{Co}(\text{NO}_3)_2$ with a concentration of 0.05

mol/L for 2 min. After drying naturally, the substrate was placed on the top of a high-purity graphic crucible (purity: 99%) containing 0.3 g precursor powders. Then the crucible with the substrate was located into the center of the graphite-heater furnace. The furnace chamber was firstly pumped to 10^{-4} pa to clear the oxygen, followed by introducing the atmosphere mixture of 5 vol% nitrogen and 95 vol% argon (both are 99.99% purity, 0.1 Mpa) into the chamber. This process was repeated for three times to reduce the concentration of O_2 to a negligible level. Then the system was heated up to the desired temperature of 1450 °C within 48 min and then cooling down to 1100°C within various times of 10, 15 and 20 min to make different cooling rates (corresponding to the cooling rates of 35, 23.3 and 17.5 °C/min, respectively), followed by furnace cooling to room temperature (ESI, Fig. S1). The resultant products were referred to the sample of S10, S15, S20, respectively. To determine a suitable cooling rate for the growth of SiC field emitters with clear and sharp tips, the growth of SiC nanoneedle arrays was also carried out to make the temperature of 1450 °C cooling down to 1100 °C within respective 18 and 25 min (corresponding to the cooling rates of 19.4 and 14 °C/min, respectively) with otherwise similar experimental conditions, and the obtained products were referred to the sample of S18 and S25, respectively.

The obtained products were characterized using field emission scanning electron microscopy (FESEM, S-4800, Hitachi, Japan), X-ray diffraction (XRD, D8 Advance, Bruker, Germany) with Cu Ka radiation ($\lambda=1.5406$) and high-resolution transmission electron microscopy (HRTEM, JEM-2100F, JEOL, Japan) equipped with energy dispersive X-ray spectroscopy (EDS, Quantax-STEM, Bruker, Germany). The FE properties of flexible SiC emitters were performed on a home-built high vacuum field emission setup with a base pressure of $\sim 1.5 \times 10^{-7}$ Pa at room temperatures. The current-voltage

(*I-V*) curves were recorded on a Keithley 248 unit with a detection resolution of 0.1 fA. The distance between the surface of SiC nanostructures and the anode of vacuum chamber was fixed at $\sim 800 \mu\text{m}$.

3. Results and Discussion

Fig. 1 (a1, b1 and c1) show the representative SEM images of S10, S15 and S20 under low magnifications, suggesting the large-scale and high density growth of the 1D SiC nanostructures with uniform size distribution (ESI, Fig. S2-4). The lengths of three samples can be up to tens of micrometers (as shown in Table 1, which are summarized from more than 30 nanowires of each sample). It should be noted that most of the nanostructures often grow in the area between two carbon fibers and stand vertically to the carbon fibers, which construct the wires into quasialigned nanoarrays. Notably, these nanoarrays are highly flexible even treated at the high-temperature of $1450 \text{ }^\circ\text{C}$ (ESI, Fig. S5).²⁵ Fig. 1(a2-c3) depict an individual SiC nanostructure obtained from S10, S15 and S20, respectively. The catalyst droplet particles could be clearly found on the tips of the S10 and S15, implying that the growth of the SiC nanowires should be governed by the vapor-liquid-solid (VLS) process.³⁰ The average sizes of the catalytic particles are gradually decreased from 636 nm to 393 nm with the increase of the cooling time from 10 min to 15 min. However, closer observation of S20 discloses that the tip of the wire is clear without any attachment of catalyst particle (as shown in Fig. 1(c3) and ESI, Fig. S4). The detailed mechanism will be discussed in the following section. It seems that the SiC nanostructures are gradually transformed from conventional nanowires into nanoneedles with the decrease of the cooling rates. The maximum diameters of S10, S15 and S20 are almost identical to each other (as shown in Table 1), suggesting the similar growth of the SiC nanowires in the initial growth stage. However, lower cooling rates could make the growth of the SiC nanoneedle arrays with sharper tips, longer lengths and larger

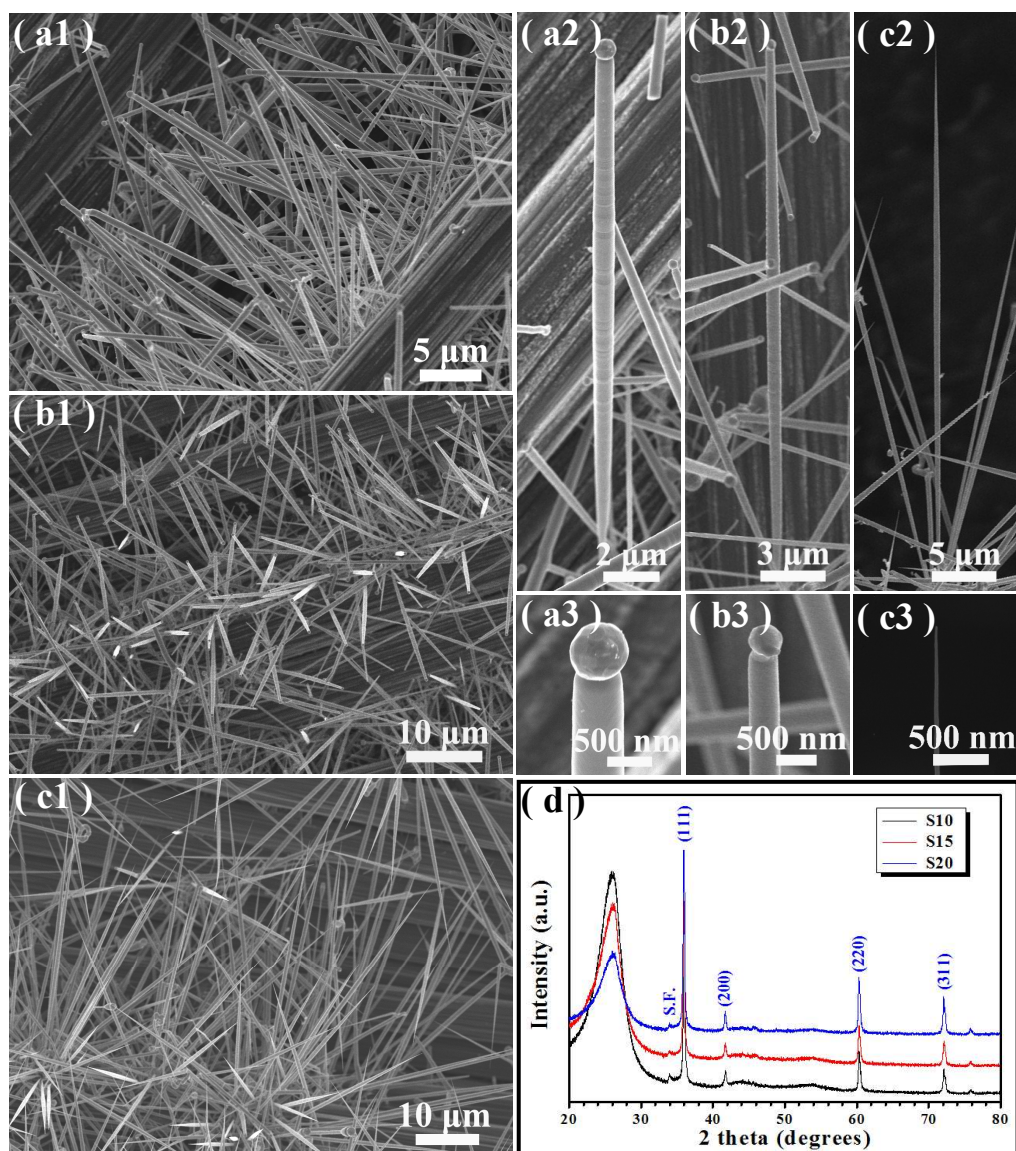


Fig. 1 Typical SEM images of as-grown quasisaligned SiC nanoarrays of S10 (a1, a2, a3), S15 (b1, b2, b3) and S20 (c1, c2, c3) under different magnifications. (d) Typical XRD pattern of the as-synthesized products of S10, S15 and S20.

Table 1 Details of the as-synthesized SiC nanoneedles of S10, S15, S20.

Samples	Diameter of catalytic particle (nm)	Maximum diameter of the nanostructures (nm)	Length of the nanostructure (μm)	Aspect ratio
S10	636	638	16.6	25.6
S15	423	624	24.7	39.6
S20	/	628	40.6	64.6

the cooling rates. Fig. 1(d) shows the typical XRD patterns of S10, S15 and S20. It discloses that, beside aspect ratios (as shown in Table 1). That is to say, in present work, the controlled growth of quasialigned SiC nanoneedle arrays could be achieved by regulating the catalytic particle sizes through the control on the cooling rates. Fig. 1(d) shows the typical XRD patterns of S10, S15 and S20. It discloses that, beside the peaks of substrate, all of the other peaks are in good agreement with the 3C-SiC (JCPDS Card No. 29-1129), disclosing that the grown quasialigned nanoneedle arrays are of pure 3C-SiC, regardless of the different cooling rates. The low intensity peak marked with "S.F." is attributed to the stacking faults within the 3C-SiC.³¹ The strong and sharp diffraction peaks indicate that the as-grown SiC nanostructures possess a good crystallinity.

The detailed structures of the as-synthesized quasialigned SiC nanoneedle arrays were further characterized by using TEM. Fig. 2(a1) is a typical TEM image near the tip of a single nanowire of S15 under a low magnification, suggesting that the diameter of nanowire gradually decreases along the length direction with a catalytic particle sized in ~430 nm in diameter on the tip, which is consistent with the SEM observations. The EDS spectrum recorded from the tip (marked area of A in Fig. 2(a1)) reveals that it mainly consists of Si, C, Co and Cu, as shown in Fig. 2(a2), suggesting that the dark particle should be serviced as the catalytic droplet. The typical EDS spectrum recorded from the body of wire discloses that the nanowire mainly consist of Si, C and N, as well as a small amount of O (ESI, Fig. S6). The O is from the amorphous SiO_x outlayer around the SiC wires, and the Cu comes from the copper grid used to support the TEM sample. The atomic ratio of Si to C, within the experimental limit, is close to 1:1, suggesting the wires are SiC. The N concentration within the wires is measured to be ~3.35 at.%. Along with the XRD analysis (Fig. 1(d)), it suggests that the quasialigned nanoneedles are

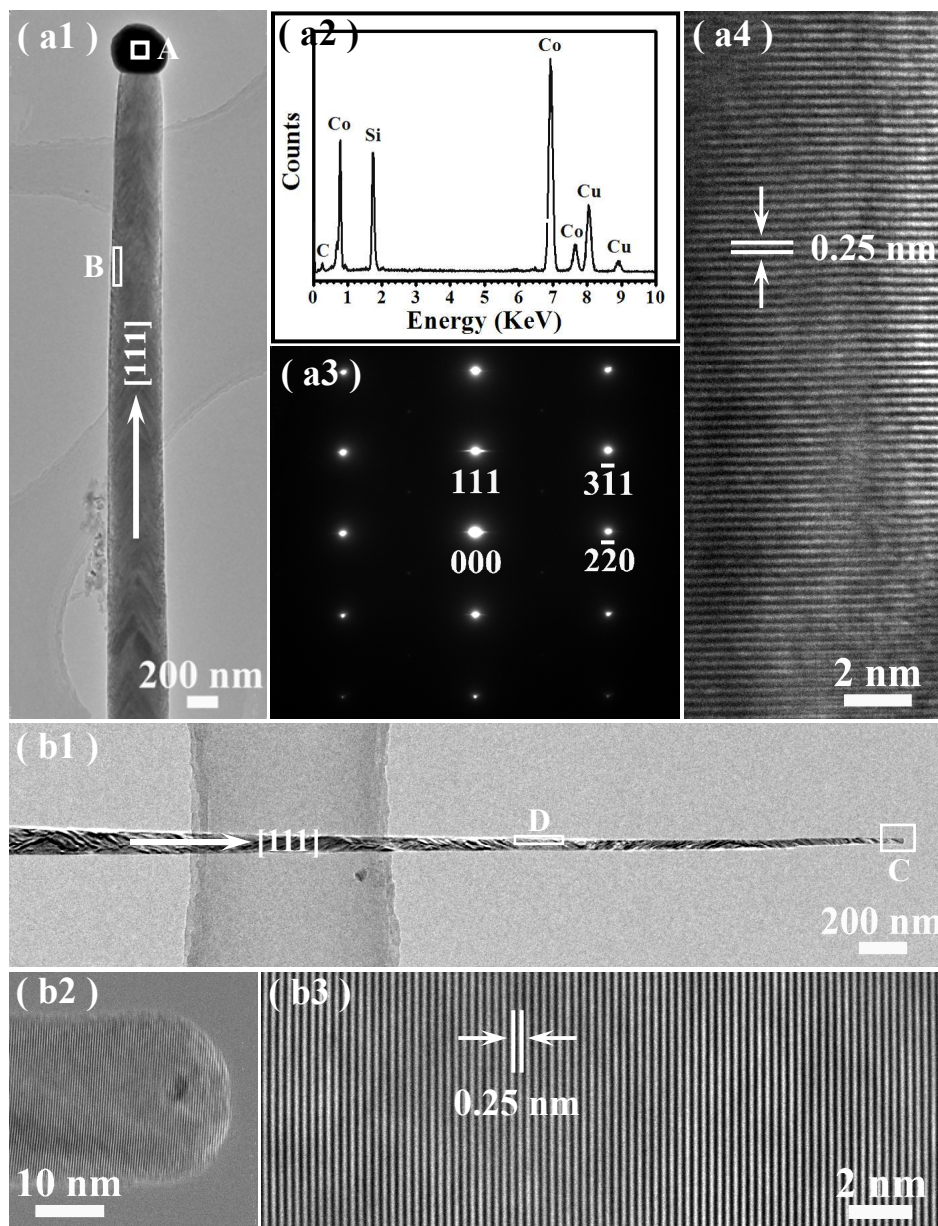


Fig. 2 (a1) A typical TEM image of the wire tip of S15 under a low magnification. (a2) A representative EDS spectrum recorded from the catalytic particle. (a3-a4) The corresponding SAED pattern and HRTEM image of the wire body of S15. (b1-b2) Typical TEM images of the wire tip of S20 under different magnifications. (b3) The corresponding HRTEM image of the wire body of S20.

composed by N-doped 3C-SiC nanowires.²⁵ Fig. 2(a3) shows the selected area electron diffraction (SAED) pattern, which is identical over the entire wires except the catalytic particle, suggesting that the nanowire is 3C-SiC (JCPDS Card No. 29-1129) with the nature of single crystal. Fig. 2(a4) presents a

HRTEM image recorded from the marked area of B in Fig. 2(a1), displaying the perfect structure with few defects of the as-synthesized SiC nanowires. The measured lattice fringe spacing of 0.25 nm responds to {111} plane distance of 3C-SiC, disclosing that the nanowire grows along the [111] direction, as indexed in Fig. 2(a1). Fig. 2(b1) is the typical TEM image near the tip part of the resultant wire of S20 under a low magnification. It demonstrates that the obtained SiC nanostructure of S20 possess a needle shape with sharp tip, which is distinctively different from that of S15. Fig. 2(b2) is the respective TEM image recorded from the marked areas of C in Fig. 2(b1), displaying the detailed structure of the tip of the SiC nanoneedle. The sharp tip is clear without any attached catalytic droplets and the diameter is only ~ 5 nm (ESI, Fig. S7). Fig. 2(c) responds to the HRTEM image of the as-synthesized nanoneedle recorded from the marked areas of D in Fig. 2(b1), indicating that the nanoneedle possesses a perfect crystal structure with few defects. These results demonstrate that obtained nanostructures are both of single-crystalline 3C-SiC, regardless of the various cooling rates used for the growth of the quasialigned nanoarrays.

The experimental results as mentioned above suggest that the cooling rates plays a key role on the formation of the nanowires with sharp tips, enabling the controlled growth of the quasialigned SiC nanoneedle arrays. Here, we proposed a mechanism based on the VLS process for the growth of SiC nanowires with sharp tips, which is schematically illustrated in Fig. 3. The PSN polymeric precursors were converted into SiCN(O) amorphous ceramics when heated up to 1000°C.³² Further increase of the temperature would result in the release of SiO and CO vapors,³³ The vapor phases of SiO and CO would react with the used catalysts of Co(NO₃)₂, leading to the formation of molten Co alloy catalytic droplets (schematically shown as step I in Fig. 3). With the increase of the temperature up to 1450 °C, the vapor

species would dissolve in the formed catalyst liquid droplets, resulting in the supersaturation of the Si and C elements. Further dissolution of SiO and CO within the catalytic droplets would make the precipitation of the Si and C elements, thus leading to the nucleation of SiC on the carbon fabric substrates (schematically shown as step II in Fig. 3). The repeated dissolution and precipitation lead to the growth of SiC nanowires (schematically shown as step III in Fig. 3). It is well known that the diameter of the nanowire should be confined by the size of the catalytic droplet. At the beginning of the growth of SiC crystals, the small size of the nuclei, compared to the large catalyst droplet, would result in a large contact angle between the nuclei and catalytic droplet, which generates an outward force (F) on the nanostructure (shown as the marked area of N in Fig. 3).³⁴ This outward force would make the lateral growth of the SiC nanowires with gradual increase in the diameter, which accounts for the tapered growth of the SiC nanowires of S10, S15 and S20 over the initial growth process of Section A in Fig. 3 (also shown in Fig. 1 and ESI, Fig. S2-4). Further lateral growth of the wires might lead to the decrease of the contact angle owing to the increase of the contact area between the nanostructure and the droplet (shown as the marked area of G and the corresponding enlarged picture of G). Once the size of the SiC nanowires is comparable to that of catalytic droplet (schematically shown as step IV in Fig. 3), the followed growth of the nanowires would be confined by the catalytic droplet, which often results in the growth of the nanowire with a constant diameter as reported in most of the previous works. However, the subsequent growth of the SiC nanowires with gradually reduced sizes in diameter could be attributed to following reasons.²⁹ The crystal nucleation and growth rely on the supersaturation, and the dissolutions of the Si and C elements in Co alloy catalytic droplets are remarkably influenced by the variation of the temperatures. This means that a decrease of the temperature might result in a lower dissolution of the vapor species within the catalytic liquid droplet, which, in turn, leads to the size

decrease of the catalytic droplet. Meanwhile, it should be noted that the sizes of the catalytic droplets are determined by two competition cases, *i.e.*, the dissolvability and vaporization of the catalytic alloy droplet induced by the changes of the temperature. A faster cooling rate suggests a higher supersaturation, leading to a faster reduce in catalytic droplets sizes; and a faster cooling rate implies a lower vaporization induced by the high temperatures, resulting in a slower reduce in catalytic droplets sizes (schematically shown as step V and VI in Fig. 3). This is supported by our experimental results that the sizes of the catalytic droplets are averagely sized in ~ 696 and ~ 423 nm (as shown in Table 1), corresponding to the pyrolysis schedules with cooling times of 10 and 15 min, respectively. The different sizes of the catalytic droplets make the growth of the wire tips of S10 and S15 with different sharp degrees (Fig. 1(a3-b3) and ESI, Fig. S2-3). Thus, further reducing the cooling rates would lead to the growth of the SiC nanowire with a sharper tip (Fig. 1). The observed clear tips of S20 (Fig. 2(b2)) could be attributed to the enough lower cooling rate, in which the alloy catalytic droplet might be completely evaporated caused by the enough long time maintained at the high temperature of 1450°C .

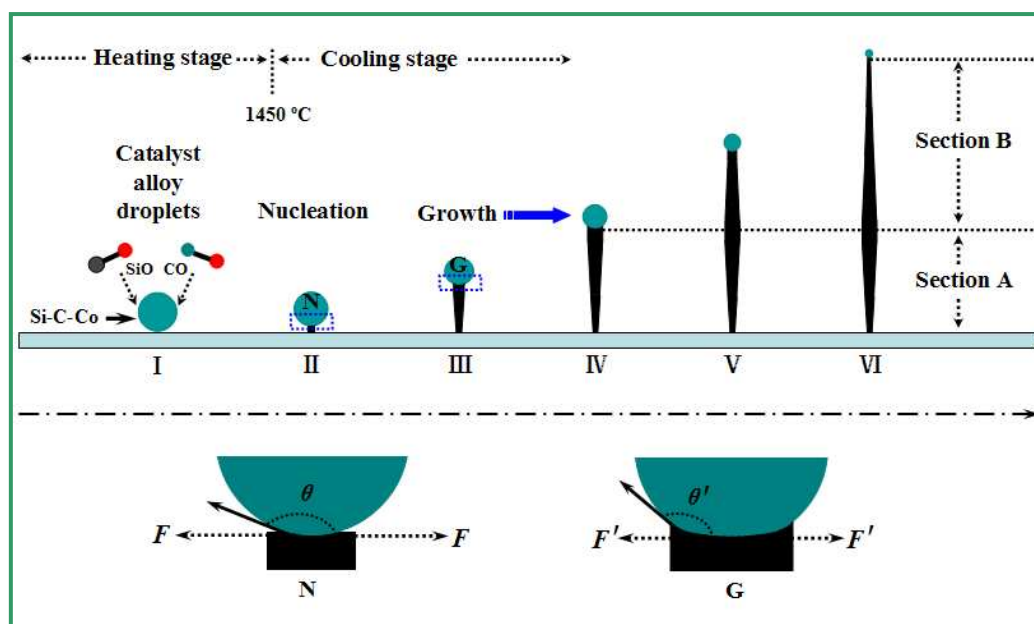


Fig. 3 Schematic illustration for the growth of SiC nanowires with tailored sharp tips based on the VLS mechanism.

These results clearly suggest that the cooling rates play a significantly important role on the growth of SiC nanowires, enabling the capability for well-controlled growth of SiC nanostructures with sharp and clear tips by adjusting the cooling rates.

To optimize the cooling rates to favor the growth of SiC nanoneedle arrays with clear and sharp tips as mentioned above, another two comparison experiments with cooling times of 18 and 25 min have also been performed (*i.e.*, samples of S18 and S25) with otherwise similar experimental conditions. Fig. 4(a1-a3) displays the typical SEM images of the obtained products of S18 under different magnifications (also shown in ESI, Fig. S8). The catalytic droplet averagely sized in ~ 60 nm is always

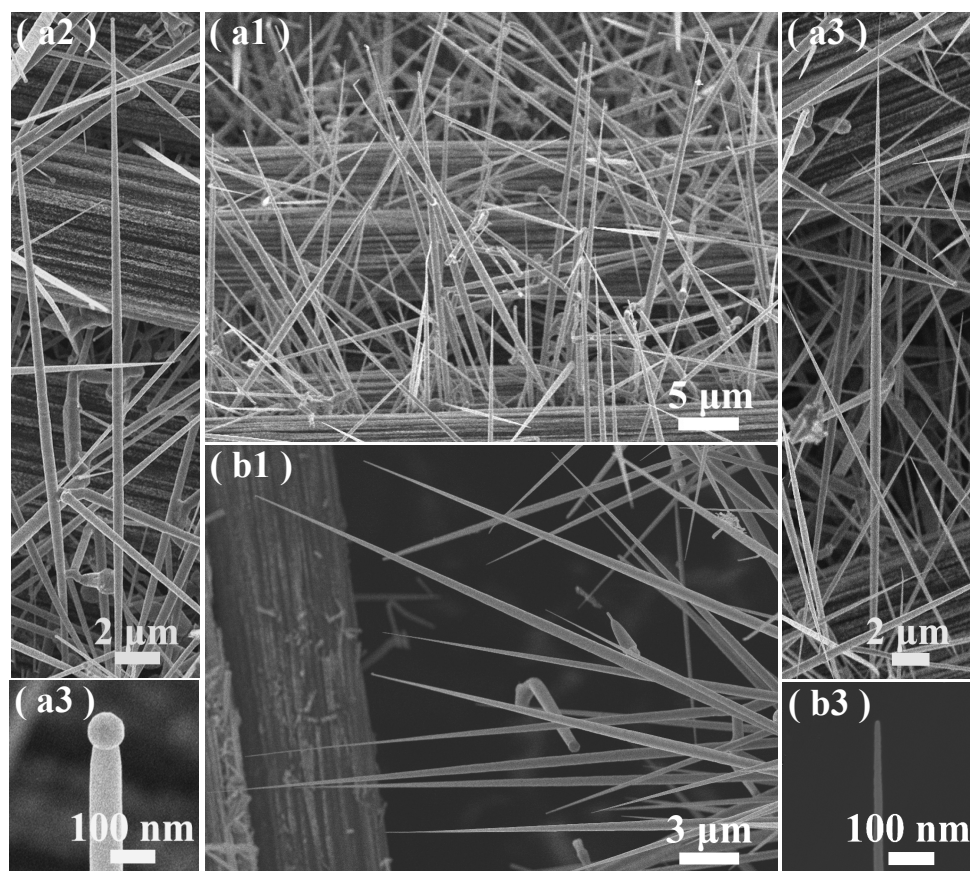


Fig. 4 Typical SEM images of as-synthesized quasialigned SiC nanoarrays of S18 (a1, a2, a3) and S25 (b1, b2, b3) under different magnifications.

observed on the tips of the wires, which is much smaller than that of S15 with an average size of ~ 423 nm. This confirms that a smaller cooling rate could lead to the formation of a smaller sized catalytic droplet, which makes the growth of SiC nanowire with a smaller diameter size, and consequently leads to the formation of the growth of the wires with a sharper tip. Fig. 4(b1-b3) depicts the typical SEM images of the resultant products of S25 (cooling rate: $14\text{ }^{\circ}\text{C}/\text{min}$) under different magnifications, suggesting the similar needle-shaped wires with a clear and sharp tip to those of S20 (also shown in ESI, Fig. S9). This means that, in current work, the catalytic droplet might be thermally evaporated completely once the cooling time is long enough up to 20 min (cooling rate: $17.5\text{ }^{\circ}\text{C}/\text{min}$), suggesting that the cooling rate of $17.5\text{ }^{\circ}\text{C}/\text{min}$ is low enough to favor the growth of the SiC flexible nanoarrays with clear and sharp tips.

Fig. 5(a) shows the field-emission current density (J) versus the applied field (E) plots for characterization of the FE performances of the obtained samples of S10, S15 and S20 in room temperature. The J - E curves were obtained after sweeping the voltage several times until the electron emission was stable. The field emission current-voltage characteristics were further analyzed based on the Fowler-Nordheim (F - N) theory³⁵, suggesting that the electron emission of the SiC emitters follows the conventional field emission mechanism (Fig. 5(b)). The turn-on fields (E_{to}) (defined to be the electric field required to generate a current density of $10\text{ }\mu\text{A}/\text{cm}^2$) are of ~ 2.19 , 2.04 and $1.15\text{ V}/\mu\text{m}$ for the samples of S10, S15 and S20, respectively. It seems that the E_{to} of S20 is markedly reduced as compared to those of S10 and S15, exhibiting the best FE performance with a E_{to} of $1.15\text{ V}/\mu\text{m}$ (Fig. 5(c)). These results demonstrate that the FE properties of the flexible SiC emitters could be profoundly enhanced by controlling the growth of SiC nanowires with clear and sharp tips, suggesting that present

work might push forward the applications of SiC one-dimensional nanostructures towards the field emitters with enhanced properties in FE display industry.

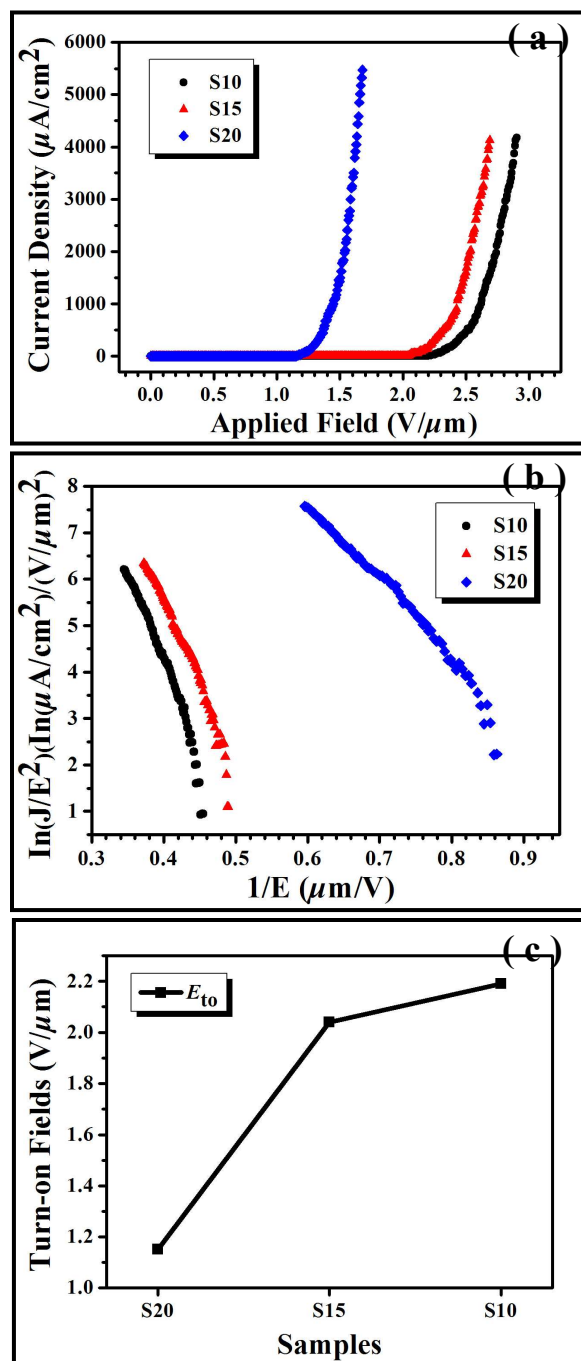


Fig. 5 FE properties of the resultant Samples of S10, S15 and S20. (a) J - E plots of obtained three samples; (b) Corresponding F-N plots of three samples; (c) The variation of E_{to} of three samples.

4. Conclusions

In summary, based on the confined growth of nanowires in the VLS mechanism, we have demonstrated the controlled growth of 3C-SiC flexible field emitters via catalyst assisted pyrolysis of polymeric precursors on the carbon fabric substrates. By reducing the cooling rates over the high-temperature pyrolysis process, the growth of the SiC nanowires with clear and sharp tips could be achieved, suggesting the well controlled growth of quasialigned SiC nanoneedle arrays. It is found the cooling rate of 17.5 °C is low enough to make the growth of SiC nanowires with unique sharp and clear tips. Moreover, lower cooling rates could favor the growth of the SiC nanoneedle arrays with sharper tips, longer lengths and larger aspect ratios. The FE properties measurements confirm that the electron emission of the flexible SiC emitters could be profoundly enhanced by controlling the growth of SiC nanowires with clear and sharp tips. It is promising that current work could push forward the practical applications of SiC one-dimensional nanostructures towards the field emitters with enhanced FE properties.

Acknowledgements

This work was supported by 973 program (Grant No. 2012CB326407), National Natural Science Foundation of China (NSFC, Grant Nos. 51072084, 51002083, 51372123 and 51232004), and Zhejiang Provincial Science Foundation for Distinguished Young Scholars (Grant No. R4100242).

Electronic supplementary information (ESI) available: SEM and TEM characterization of the synthesized quasialigned SiC nanoneedle arrays. See DOI: xxxxxxxxxx

References

1. Z. L. Wang, *Adv. Mater.*, 2003, **15**, 432.
2. Y. Xia, P. Yang, Y. Sun, Y. Wu, B. Mayers, B. Gates, Y. Yin, F. Kim and H. Yan, *Adv. Mater.*, 2003, **15**, 353.
3. P. Yang, R. Yan and M. Fardy, *Nano Lett.*, 2010, **10**, 1529.
4. T. Zhai, L. Li, Y. Ma, M. Liao, X. Wang, X. Fang, J. Yao, Y. Bando and D. Golberg, *Chem. Soc. Rev.*, 2011, **40**, 2986.
5. K. Zekentes and K. Rogdakis, *J. Phys. D: Appl. Phys.*, 2011, **44**, 133001.
6. R. Wu, K. Zhou, J. Wei, Y. Huang, F. Su, J. Chen and L. Wang, *J. Phys. Chem. C*, 2012, **116**, 12940.
7. R. Shao, K. Zheng, Y. Zhang, Y. Li, Z. Zhang and X. Han, *Appl. Phys. Lett.*, 2012, **101**, 233109.
8. J. Fan, X. Wu and P. K. Chu, *Prog. Mater. Sci.*, 2006, **51**, 983.
9. E. W. Wong, P. E. Sheehan and C. M. Lieber, *Science*, 1997, **277**, 1971.
10. J. Bi, G. Wei, L. Wang, F. Gao, J. Zheng, B. Tang and W. Yang, *J. Mater. Chem. C*, 2013, **1**, 4514.
11. F. Gao, J. Zheng, M. Wang, G. Wei and W. Yang, *Chem. Commun.*, 2011, **47**, 11993.
12. W. Zhou, X. Liu and Y. Zhang, *Appl. Phys. Lett.*, 2006, **89**, 223124.
13. G. Wei, H. Liu, C. Shi, F. Gao, J. Zheng, G. Wei and W. Yang, *J. Phys. Chem. C*, 2011, **115**, 13063.
14. H. Cui, Y. Sun, G. Yang, J. Chen, D. Jiang and C. Wang, *Chem. Commun.*, 2009, 6243.
15. Z. Li, W. Ren and A. Meng, *Appl. Phys. Lett.*, 2010, **97**, 263117.
16. H. Cui, L. Gong, G. Yang, Y. Sun, J. Chen and C. Wang, *Phys. Chem. Chem. Phys.*, 2011, **13**, 985.
17. G. Shen, Y. Bando, C. Ye, B. Liu and D. Golberg, *Nanotechnology*, 2006, **17**, 3468.
18. M. G. Kang, H. J. Lezec and F. Sharifi, *Nanotechnology*, 2013, **24**, 065201.
19. Z. Pan, H. L. Lai, F. C. Au, X. Duan, W. Zhou, W. Shi, N. Wang, C. S. Lee, N. B. Wong and S. T. Lee, *Adv. Mater.*, 2000, **12**, 1186.
20. Y. Tang, H. Cong, Z. Chen and H. Cheng, *Appl. Phys. Lett.*, 2005, **86**, 233104.
21. J. O. Hwang, D. H. Lee, J. Y. Kim, T. H. Han, B. H. Kim, M. Park, K. No and S. O. Kim, *J. Mater. Chem.*, 2011, **21**, 3432.
22. X. Wang, J. Zhou, C. Lao, J. Song, N. Xu and Z. L. Wang, *Adv. Mater.*, 2007, **19**, 1627.
23. J. H. He, R. Yang, Y. L. Chueh, L. J. Chou, L. J. Chen and Z. L. Wang, *Adv. Mater.*, 2006, **18**, 650.

24. X. Fang, Y. Bando, U. K. Gautam, C. Ye and D. Golberg, *J. Mater. Chem.*, 2008, **18**, 509.
25. S. Chen, P. Ying, L. Wang, G. Wei, J. Zheng, F. Gao, S. Su and W. Yang, *J. Mater. Chem. C*, 2013, **1**, 4779.
26. J. Huang, K. Kempa, S. Jo, S. Chen and Z. Ren, *Appl. Phys. Lett.*, 2005, **87**, 053110.
27. P. Ghosh, M. Z. Yusop, S. Satoh, M. Subramanian, A. Hayashi, Y. Hayashi and M. Tanemura, *J. Am. Chem. Soc.*, 2010, **132**, 4034.
28. H. Wang, Z. Xie, W. Yang, J. Fang and L. An, *Cryst. Growth Des.*, 2008, **8**, 3893.
29. W. Feng, J. Ma and W. Yang, *CrystEngComm*, 2012, **14**, 1210.
30. R. Wagner and W. Ellis, *Appl. Phys. Lett.*, 1964, **4**, 89.
31. K. Koumoto, S. Takeda, C. H. Pai, T. Sato and H. Yanagida, *J. Am. Ceram. Soc.*, 1989, **72**, 1985.
32. A. Dhamne, W. Xu, B. G. Fookes, Y. Fan, L. Zhang, S. Burton, J. Hu, J. Ford and L. An, *J. Am. Ceram. Soc.*, 2005, **88**, 2415.
33. Y. Li, Y. Liang and Z. Hu, *Ceram. Int.*, 1995, **21**, 59.
34. F. Ross, J. Tersoff and M. Reuter, *Phys. Rev. Lett.*, 2005, **95**, 146104.
35. R. H. Fowler and L. Nordheim, *Proc. R. Soc. London, Ser. A*, 1928, **119**, 173.